JOURNAL OF GEOPHYSICAL RESEARCH, VOL. 106, NO. D1, PAGES 1297–1309, JANUARY 16, 2001

Mechanisms for midlatitude ozone loss: Heterogeneous chemistry in the lowermost stratosphere?

Jessica B. Smith, Eric J. Hintsa,[1] Norton T. Allen,
Richard M. Stimpfle and James G. Anderson

Department of Chemistry and Chemical Biology, Harvard University, Cambridge, Massachusetts

Abstract. The question of midlatitude ozone erosion by chlorine free radical catalysis is examined. We present and analyze simultaneous, high-resolution observations of ClO, H_2O, tropopause height, particle reactive surface area, and ice saturation occurrence frequency obtained from the NASA ER-2 aircraft. The objective is to test the hypothesis that the existence of cirrus clouds or cold aerosols in the first few kilometers above the tropopause at midlatitudes is responsible for increasing the ratio of chlorine free radicals to total inorganic chlorine, thus amplifying the rate of catalytic ozone destruction. The observations reveal a sharp decrease in ice saturation frequency at the tropopause, a marked degree of undersaturation just above the tropopause, a corresponding sharp gradient in the product of cold aerosol reactive surface area and reaction probability, γS_a, and, finally, the consistent absence of enhanced concentrations of ClO immediately above the tropopause. These results suggest that midlatitude ozone loss is not controlled in situ by the mechanism of cirrus cloud and/or cold aerosol enhancement of chlorine radicals in the vicinity of the tropopause.

1. Introduction

Losses of ozone over midlatitudes of the northern hemisphere are well documented in both the scientific literature and the public policy arena. Accurately defining secular trends in the vertical distribution of ozone, and establishing the mechanism responsible for the observed losses are two dominant and enduring issues. Considerable progress has recently been made with respect to determining ozone trends. In an analysis of global ozonesonde stations, *Logan et al.* [1999, p. 26,373] report "significant decreases in stratospheric ozone at all stations in middle and high latitudes of the northern hemisphere from 1970 to 1996, with the largest decreases located between 12 and 21 km, and trends of -3 to -10%/decade near 17 km." They report the largest ozone losses in the late winter and spring and in the lowermost stratosphere. These results are summarized in Figure 1, which displays the seasonal mean profiles for sonde stations between 36°-53°N calculated from data collected from 1970 to 1996. *Bojkov and Fioletov* [1997] reduce the uncertainty of calculated trends in the lowermost stratosphere by analyzing ozone changes as a function of altitude from the locally determined tropopause. Their analysis shows that the negative stratospheric trends become significant 1-2 km above the tropopause. In this paper, it is the proposed mechanisms responsible for the observed ozone erosion that concern us.

The changes to midlatitude ozone are largely centered in the "lowermost stratosphere" [*Holton et al.*, 1995], the region bounded at the top by the potential temperature surface corresponding to the tropical tropopause (~380 K) and at the lower extreme by the local tropopause. Plate 1a shows a superposition of the mean annual midlatitude ozone trend, calculated by *Logan et al.* [1999], with a meridional cross section of the structure and dynamics of the troposphere and stratosphere in a framework of pressure, altitude, and potential temperature.

The predominance of ozone loss in the lowermost stratosphere presents a problem with both chemical and dynamical components because of the long chemical lifetime of ozone in that altitude region. It also critically involves the question of residence time of air in the lowermost stratosphere. Given that residence times in this region are ~6 months or less [*Rosenlof and Holton*, 1993; *Hintsa et al.*, 1998], that the region is dynamically coupled to high latitudes, and that ozone is rapidly destroyed at high latitudes in the winter and early spring, these coupled chemical and dynamical considerations are almost certainly important. However, those issues will be addressed in a subsequent publication; the emphasis in this analysis is on (1) chemical mechanisms occurring in situ at midlatitudes that could be responsible for the observed changes, and (2) high spatial and temporal resolution observations obtained primarily from the NASA ER-2 that can be used to test proposed mechanisms. Our emphasis is on observations of the water-temperature relationships in this region that define the existence of cirrus clouds and cold liquid aerosols, on the heterogeneous processes that alter the radical-molecule partitioning in this region, and on observations of the free radicals that rate limit catalytic ozone loss processes.

We examine the evidence for the existence of cirrus clouds and cold aerosols in the lowermost stratosphere, look for evidence of enhanced free radical concentrations in this region, and consider the proposal by *Solomon et al.* [1997] and [1998] that cirrus clouds and/or cold aerosols act to

[1]Now at Department of Marine Chemistry and Geochemistry, Woods Hole Oceanographic Institution, Wood Hole, Massachusetts.

Copyright 2001 by the American Geophysical Union.

Paper number 2000JD900464.
0148-0227/01/2000JD900464$09.00

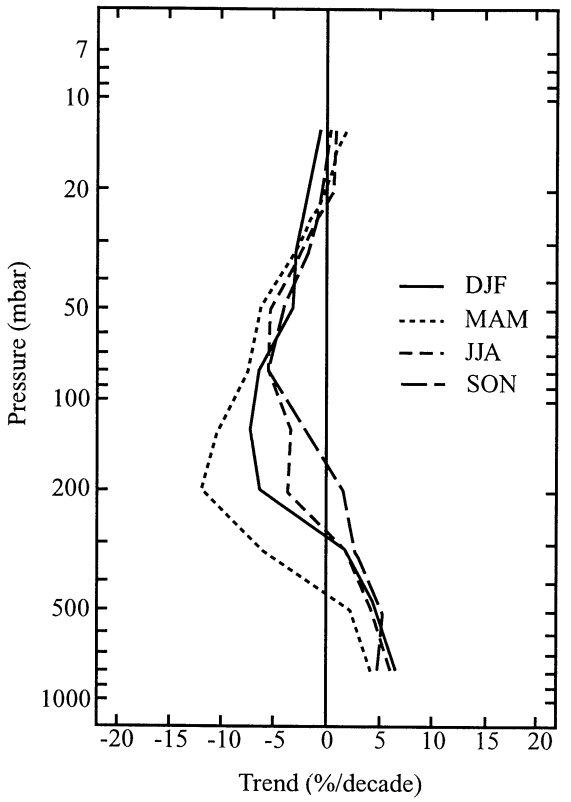

Figure 1. Seasonal mean ozone trend profiles for ozonesonde stations located between 36°-53°N. Adapted from *Logan et al.* [1999, Figure 13].

increase the ratio of halogen radicals to total inorganic halogens enough to make a significant contribution to the catalytic destruction of ozone at midlatitudes.

2. Chemical Processes and Rate-Limiting Radical Concentrations

The catalytic loss of ozone in the lower stratosphere at midlatitudes has been shown to be controlled by a combination of cycles rate limited by HO_2, ClO, BrO, and NO_2 [*Wennberg et al.*, 1994; *Stimpfle et al.*, 1999]. In particular, the catalytic destruction of ozone is rate-limited by

$$HO_2 + O_3 \rightarrow OH + O_2 + O_2 \text{ in the } HO_x \text{ cycle} \quad (1)$$

$$NO_2 + O \rightarrow NO + O_2 \text{ in the } NO_x \text{ cycle} \quad (2)$$

and

$$ClO + O \rightarrow O_2$$
$$ClO + HO_2 \rightarrow HOCl + O_2$$
$$ClO + NO_2 \rightarrow ClONO_2$$
$$ClO + BrO \rightarrow Cl + Br + O_2$$
$$BrO + HO_2 \rightarrow HOBr + O_2$$
$$BrO + O \rightarrow Br + O_2$$
$$BrO + NO_2 \rightarrow BrONO_2 \text{ in the } ClO_x/BrO_x \text{ cycle.} \quad (3)$$

In situ observations of the rate-limiting free radicals in the middle/lower stratosphere by the ER-2 have provided the following conclusions:

1. The dominant loss mechanism for midlatitude ozone at altitudes of 21 km and below, the region of interest here, is rate-limited by hydrogen radicals, as reported by *Wennberg et al.* [1994]. There is, however, a large seasonal variation in the fractional contribution of the HO_x ($OH + HO_2$) catalyzed loss process. In particular, because of the demonstrated NO_x ($NO_x \equiv NO + NO_2$) control over the fraction of HO_x tied up in the rate limiting radical, HO_2, [*Wennberg et al.*, 1994; T. F. Hanisco et al., Sources, sinks, and the distribution of OH in the lower stratosphere, submitted to *J. Phys. Chem.*, 2000; E. L. Lanzendorf et al., Establishing the dependence of $[HO_2]/[OH]$ on temperature, halogen loading, O_3, and NO_x based on in situ measurements from the NASA ER-2, submitted to *J. Phys. Chem.*, 2000] and because of the strong heterogeneous control over the NO_x to NO_y ratio [*Fahey et al.*, 1993], the system is both extremely nonlinear and highly sensitive to the balance between insolation and the rate of N_2O_5 hydrolysis, the heterogeneous reaction that dominates the conversion of NO_x to NO_y ($NO_y \equiv HNO_3 + HNO_4 + 2N_2O_5 + NO_x + NO_3 + ClONO_2 + BrONO_2 + \ldots$).

2. Halogen radicals play a significant role in this region and they too are highly sensitive to latitude, altitude, and season. This is, of course, most dramatically evident at high latitudes in the winter and early spring [*Brune et al.*, 1991; *Toohey et al.*, 1993] when halogen-catalyzed ozone loss not only exceeds other catalytic cycles, but is amplified such that ozone lifetimes drop from months to weeks [*Anderson et al.*, 1991]. In sharp contrast to the late winter/early spring conditions, high-latitude summer conditions reflect the dominance of gas phase reactions coupled with 24-hour illumination that serves to amplify the concentrations of NO and NO_2 [*Del Negro et al.*, 1999; K. K. Perkins et al., The NO_x-HNO_3 system in the lower stratosphere: Insights from in situ measurements and implications of the J_{HNO3}-OH relationship, submitted to *J. Phys. Chem.*, 2000], thereby suppressing the concentrations of the halogen rate-limiting radicals, particularly ClO [*Stimpfle et al.*, 1999].

3. The role of nitrogen radicals shifts from the primary "buffering agent" at subtropical and mid/high latitudes, where the primary rate-limiting radical concentrations, $[HO_2]$ and [ClO], are the dominant catalytic agents, which decrease rapidly and nonlinearly with increasing $[NO_x]$ to the primary "catalytic agent" at high latitudes in summer where intense and nearly continuous insolation overwhelms the heterogeneous loss of NO_x to HNO_3 and leaves NO_2 the primary rate-limiting radical in the photochemical destruction of ozone.

Measured concentrations of the radicals involved in each of the rate-limiting steps defined in equations (1)-(3), above, permit calculation of the lifetime of ozone against catalytic destruction by the dominant cycles. This is done to first order by dividing the ozone concentration in the midlatitude lower stratosphere by the sum of the rate-limiting steps, that is, the loss rate of ozone:

$$\begin{aligned} -d[O_3]/dt = {} & \underbrace{2k_{NO2+O}[NO_2][O]}_{NO_x \text{ catalysis}} + \underbrace{2k_{HO2+O3}[HO_2][O_3]}_{HO_x \text{ catalysis}} \\ & + 2k_{ClO+O}[ClO][O] + 2k_{ClO+HO2}[ClO][HO_2] \\ & + 2k_{BrO+O}[BrO][O] + 2k_{BrO+HO2}[BrO][HO_2] \\ & + 2k_{ClO+BrO}[ClO][BrO] \\ & \Big\} ClO_x/BrO_x \text{ catalysis} \\ & + \text{minor terms involving } ClONO_2 \\ & \quad \text{and } BrONO_2 \text{ photolysis.} \end{aligned} \quad (4)$$

Outside of high-latitude winter/spring, this yields a lifetime for ozone against photochemical loss in the lowermost stratosphere in the range of 1 year to many years, depending on latitude and season. This is considerably longer than

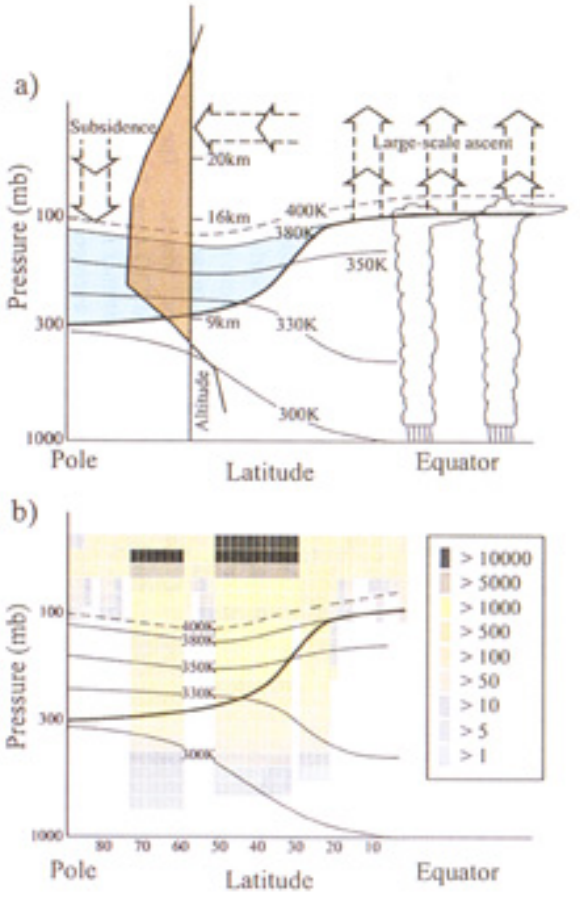

Plate 1. (a) Superposition of the annual mean midlatitude ozone trend (shaded red) with a meridional cross section of the structure and dynamics of the stratosphere/ troposphere. The ozone loss profile is located using the relationship between pressure, altitude, and potential temperature at midlatitudes. The "lowermost stratosphere" (shaded blue) is the region between the tropopause (thick black line) and the 380 K surface; the "overworld" is the region above 380 K. (b) Effective sampling area of the ER-2 during STRAT and POLARIS missions. The structural schematic of the stratosphere and troposphere is included for reference. The large variability in the position of the subtropical jet and the "tropopause break" increases our atmospheric sampling range from ~7° latitude, centered around Moffett Field (37°N), to ~20°. The color bar denotes the number of observations in each altitude/ latitude bin.

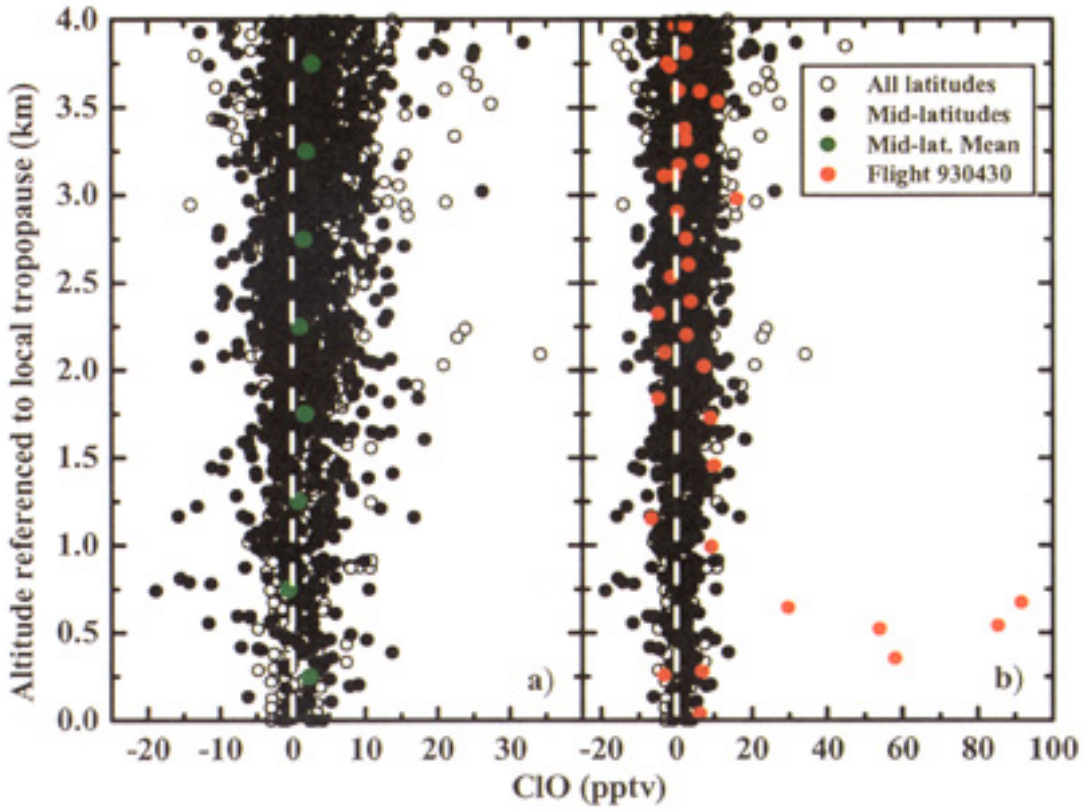

Plate 2. (a) Plot of ClO, measured aboard the ER-2 during the SPADE (except the flight of April 30, 1993), ASHOE/MAESA, and POLARIS missions, as a function of altitude above the tropopause. The midlatitude (30°-50°N/S) data are plotted in black; data from all other latitudes are open circles. The midlatitude means, evaluated for each 0.5 km bin, are plotted in green. (b) Plot of ClO data with the inclusion of the April 30, 1993, flight in red.

estimates of the timescale for transport. Because we are focused here on decade-scale changes in the ozone concentration in the lower stratosphere, there are three possibilities:

1. Changes to the chemical composition of the lowermost stratosphere have occurred such that the rate of ozone loss by the catalytic cycles in equation (4) has increased, driving down ozone concentrations in this region.
2. The dynamical structure of the atmosphere has changed such that ozone is removed by transport processes more rapidly from the midlatitude lowermost stratosphere or is supplied more slowly relative to conditions in previous decades.
3. Ozone is destroyed elsewhere in the system, and those volume elements depleted in ozone are transported into the midlatitude lowermost stratosphere.

Although each of these possibilities requires careful consideration, we restrict our discussion here to the first of the three.

3. Change in Free Radical Concentration in the Midlatitude Lower Stratosphere Induced by Cirrus Clouds

Borrmann et al. [1996, 1997] proposed that cirrus cloud surfaces in the vicinity of the tropopause, composed of water ice or liquid sulfuric acid/water supercooled droplets, might activate chlorine via heterogeneous processing, and subsequently lead to ozone depletion. *Solomon et al.* [1997] offered a more detailed examination of the chemistry of the tropopause region. Using Stratospheric Aerosol and Gas Experiment II (SAGE) satellite observations and modeling, they advance the hypothesis that heterogeneous reactions on cirrus clouds and/or liquid aerosols in the vicinity of the tropopause could enhance local ClO mixing ratios by up to a factor of 30 near the tropopause at midlatitudes. They state that if cirrus clouds occur with sufficient frequency and spatial extent, they could considerably influence not only the chemical composition, but also the loss rate of ozone in the region near the tropopause. *Solomon et al.* [1997] infer

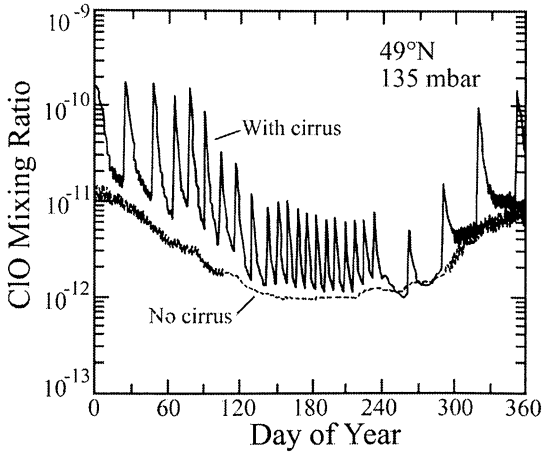

Figure 2. ClO mixing ratio in the tropopause region calculated by the *Solomon et al.* [1997] model. The solid line shows the modeled response of ClO to the presence of inferred cirrus clouds. Adapted from *Solomon et al.* [1997, Figure 7].

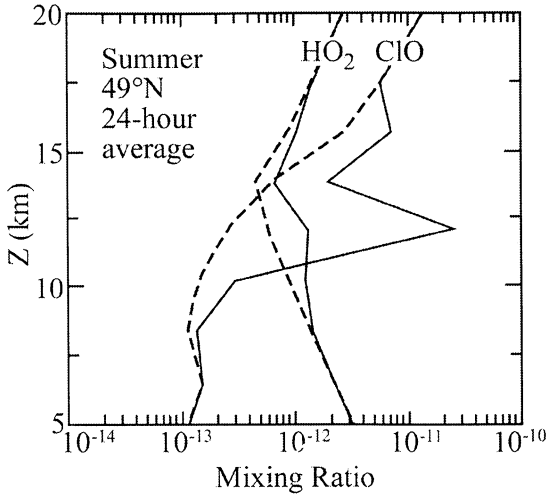

Figure 3. Diurnally averaged ClO and HO_2 profiles from 5-20 km at 49°N in summer calculated by the *Solomon et al.* [1997] model. Solid and dashed lines show calculations with and without cirrus clouds, respectively. Adapted from *Solomon et al.* [1997, Figure 14].

stratospheric cirrus cloud frequencies and surface areas from satellite observations of cloud optical depths and a climatological, or seasonally averaged, tropopause altitude, and then calculate the episodic enhancements of ClO that result from the enhanced surface area using a two-dimensional numerical model of the chemistry and dynamics of the atmosphere. The key heterogeneous reactions that occur on the inferred cirrus are,

$$HCl + ClONO_2 \rightarrow Cl_2 + HNO_3$$
$$HCl + HOCl \rightarrow Cl_2 + H_2O$$
$$H_2O + ClONO_2 \rightarrow HOCl + HNO_3$$
$$HCl + HOBr \rightarrow H_2O + BrCl.$$

Given that ClO is the rate-limiting radical in halogen-catalyzed ozone loss, the issue centers on whether these heterogeneous reactions amplify ClO concentrations in the vicinity of the tropopause enough to significantly affect ozone loss in this region. Specifically, the integrated enhancement of ClO concentrations must be sufficient to substantially increase the photochemical loss rate of ozone, and make the resulting photochemical lifetime of ozone competitive relative to transport in and out of the lowermost stratosphere. Figure 2 summarizes the *Solomon et al.* [1997] results (their Figure 7), capturing the modeled, oscillatory behavior of ClO just above the tropopause at midlatitudes that results from estimates of cirrus cloud/reactive surface area occurrence based on satellite observations. These results show both the magnitude and frequency of ClO enhancements required to account for the observed ozone trends. The altitude dependence of the cirrus-enhanced ClO from *Solomon et al.* [1997] is shown in Figure 3 for summer midlatitudes (49°N). The figure indicates that diurnally averaged ClO mixing ratios reach 25 parts per trillion by volume (pptv), which translates into noontime enhancements of ClO of approximately 50 pptv. We turn now to the question of what the high-resolution observations obtained from the NASA ER-2 contribute to this issue: Is there evidence of cirrus and/or significant ClO enhancement in the midlatitude lowermost

stratosphere? We look at the evidence of ice saturation and aerosol enhancement in the lowermost stratosphere and for measurable perturbations to the concentration of ClO, the dominant rate-limiting free radical, using flight data from a series of campaigns extending from 1993-1997 that covered latitudes from 70°S to 90°N and each of the four seasons.

4. Evidence From High-Resolution Aircraft Observations

The ER-2 aircraft provides a platform for high-resolution, in situ measurements of a host of chemical species and families. The following analysis uses data from 63 flights obtained during the Stratospheric Tracers of Atmospheric Transport (STRAT) and Photochemistry of Ozone Loss in the Arctic Region in Summer (POLARIS) missions. These missions covered the period from May 1995 through September 1997, and were flown out of NASA Ames Research Center, Moffett Field, California (37°N); Fort Wainwright Army Base, Fairbanks, Alaska (65°N); and Barbers Point Naval Air Station, Barbers Point, Hawaii (24°N). Plate 1b shows the sampling area of the stratosphere during these missions, with the structural schematic of the stratosphere and troposphere included for reference. Although all midlatitude ascents, descents, and stairstep flights from Moffett Field are geographically centered about 37°N, with a range of ~7°, our effective atmospheric sampling is significantly wider, with a range of ~20°, because of the large day-to-day variability in the latitudinal position of the subtropical jet and the tropopause.

4.1. Cloud Occurrence Frequency

The data allow for precise determination of the occurrence frequency of ice saturation, measurement of its vertical extent, and characterization of the air during such events. The flight data were binned by latitude: 0°-30°N constituted equatorial/subtropical data; 30°-50°N midlatitude data; and 50°-90°N polar data. Figure 4 shows the percentage of observations of ice saturation, evaluated for midlatitude data, as a function of altitude referenced to the measured tropopause. We used the following method: Since the height of the tropopause can vary dramatically over short timescales, we referenced the altitude associated with each data point to the local tropopause. Tropopause heights are reported for every flight (B. Gary, personal communication, 1999), and are determined using temperature and altitude values from combinations of Meteorological Measurement System (MMS) [*Scott et al.*, 1990], Microwave Temperature Profiler (MTP) [*Denning et al.*, 1989], and radiosonde data. The tropopause is calculated using the standard World Meteorological Organization (WMO) definition: the lowest altitude at which the thermal lapse rate ($-dT/dz$) is 2 K/km or smaller for all layers bounded by the candidate tropopause altitude and all altitudes within the next higher 2 km. The uncertainty associated with the tropopause calculations is typically ±0.1-0.3 km. The number of tropopause values reported per flight depends on local meteorology and the flight profile, but is typically two, one each for ascent and descent. We divide the data set for each flight accordingly and redefine altitude to kilometers above (plus) or below (minus) the observed tropopause position, and then sort the data into 0.5 km altitude bins from -5 km to +5 km about the measured tropopause position. Because

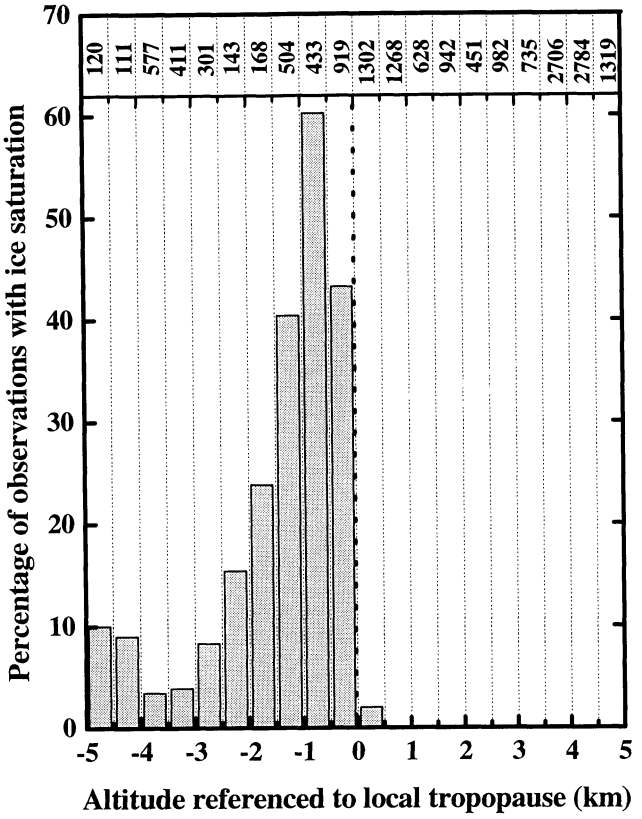

Figure 4. Histogram displaying the percentage of observations of ice saturation, evaluated for midlatitude data only (30°-50°N), as a function of altitude referenced to the measured local tropopause. The total number of observations for each 0.5 km altitude bin is shown in the corresponding box at the top.

clouds are composed primarily of water-ice particles, we expect the observation of water vapor/ice saturation to be coincident with cloud occurrence (a generous criterion, as significant supersaturation may be required to actually form clouds). Thus, in this analysis, the ratio of data points showing saturation to the total number of data points in each 0.5 km altitude bin defines the frequency of cloud occurrence. A data point is taken to indicate saturation if the measured temperature is up to 1 K warmer than the water vapor/ice saturation temperature calculated from the measured water vapor mixing ratio and measured pressure. The equation is derived from the water vapor saturation pressure over ice data in the *CRC Handbook of Chemistry and Physics* [*Weast*, 1973; *Dessler et al.*, 1995]. Again, this is a generous criterion for saturation. At saturation, 1 K at stratospheric temperatures and pressures corresponds to a change of approximately 15% in water vapor. The Harvard water vapor instrument reports data with an estimated 5% accuracy [*Hintsa et al.*, 1999], while the accuracy of temperature and pressure are ~1 K and ±0.3 mbar, respectively. A recent analysis and comparison of water vapor in the lowermost stratosphere shows reasonable agreement between data from our instrument and satellite measurements in this region [*Pan et al.*, 2000].

The midlatitude histogram in Figure 4 shows cloud occurrence frequencies building with altitude in the upper

troposphere, reaching 60% just below the tropopause, but dropping abruptly to 2% within the first 0.5 km above the tropopause. In over 1200 midlatitude measurements in the next 0.5 km altitude bin, there is no evidence of saturation. The same is true for all subsequent altitude bins. Results from the ER-2 do not support the existence of stratospheric cirrus.

Cirrus clouds have been occasionally observed in the stratosphere, but these observations have been sporadic, just above the tropopause, and largely in the tropics [*Jensen et al.*, 1996; *Beyerle et al.*, 1998; *Rinsland et al.*, 1998; *Winker and Trepte*, 1998]. *Poulida et al.* [1996] observed overshoot from an intense thunderstorm leading to clouds in the midlatitude stratosphere. However, these clouds were accompanied by largely tropospheric air with low ozone, and their lifetime was likely short before they returned to the troposphere. Thus these observations are consistent with our finding that ice saturation is extremely rare in the midlatitude stratosphere more than 500 m above the tropopause.

To further explore the possibility of ice saturation in the lowermost stratosphere, we used the time and position of selected data points/air parcels and the National Centers for Environmental Prediction (NCEP) analyses of balanced winds to calculate air parcel trajectories. The trajectory output includes the position and temperature of the specified air parcel for the previous 10 days. Whether or not the air parcel encountered saturation conditions in the past can be determined assuming the water vapor mixing ratio of the air parcel remains constant over the 10-day period. We ran back trajectories on data points selected for their saturation potential, that is, data points in the lowermost stratosphere, between 1-3 km above the local tropopause, with a separation of 10 K or less between the measured temperature and the calculated temperature of saturation. About 0.5% of the data points in that altitude range met the criterion, and we ran 10 back trajectory calculations. The back trajectories showed no evidence of prior saturation. In every case the degree of separation between the back trajectory temperature and the temperature of saturation was significantly larger than temperature fluctuations on the trajectory.

4.2. Water Vapor and Temperature in the Lower Stratosphere

The observed absence of ice saturation in the lowermost stratosphere may be understood by examining the behavior of water vapor and temperature in the upper troposphere/lower stratosphere. Relative humidity falls off by an order of magnitude immediately above the tropopause, from values close to 100% in the upper troposphere to values below 10% in the first km of the lower stratosphere, except where the upper troposphere is already dry. Figure 5 shows vertical profiles of both the measured water vapor mixing ratio and the calculated saturation mixing ratio that are typical at midlatitudes. This plot of descent into Moffett Field, California, on February 1, 1996, is representative. The dryness of air as low as 1 km above the tropopause explains the scant supply of points fulfilling our back trajectory criteria. The plot captures the following points: (1) as altitude increases above the tropopause (within the first 0.5 km), there is a transition to much lower water vapor mixing ratios; and (2) the measured temperature at the tropopause usually remains constant or increases, driving the lowermost stratosphere further from saturation.

Figure 6 consists of a series of histograms showing normalized distributions of the degrees of undersaturation, $T_{saturation} - T_{measured}$, for altitude bins from 3 km below to 3 km above the tropopause. The number of observations in each $T_{saturation} - T_{measured}$ degree bin is divided by the total number of observations, and multiplied by 100 to yield a percentage, or

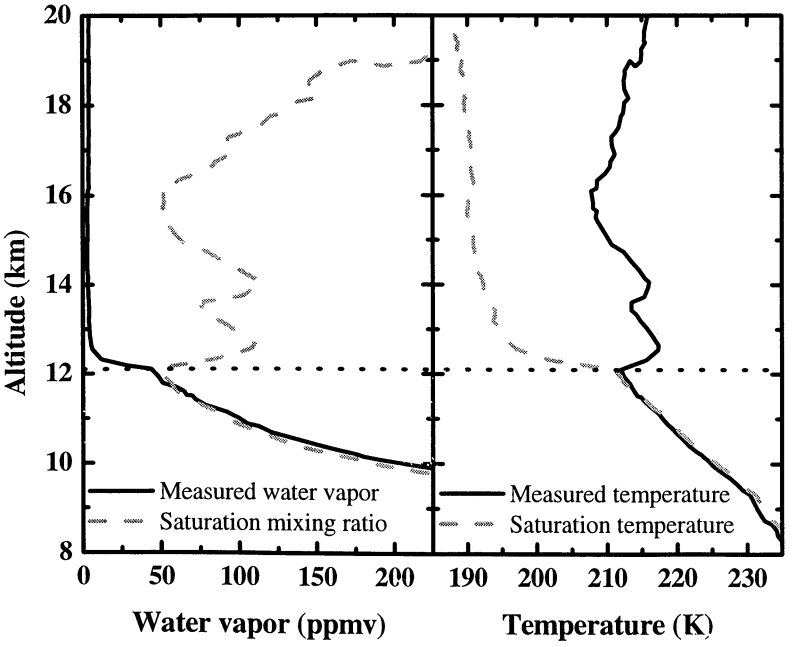

Figure 5. Conditions near the tropopause for descent into Moffett Field, California, on February 1, 1996. Measured temperature and water vapor are solid curves. Temperature of saturation and water vapor saturation mixing ratio are dashed curves. The horizontal dotted line indicates the position of the tropopause.

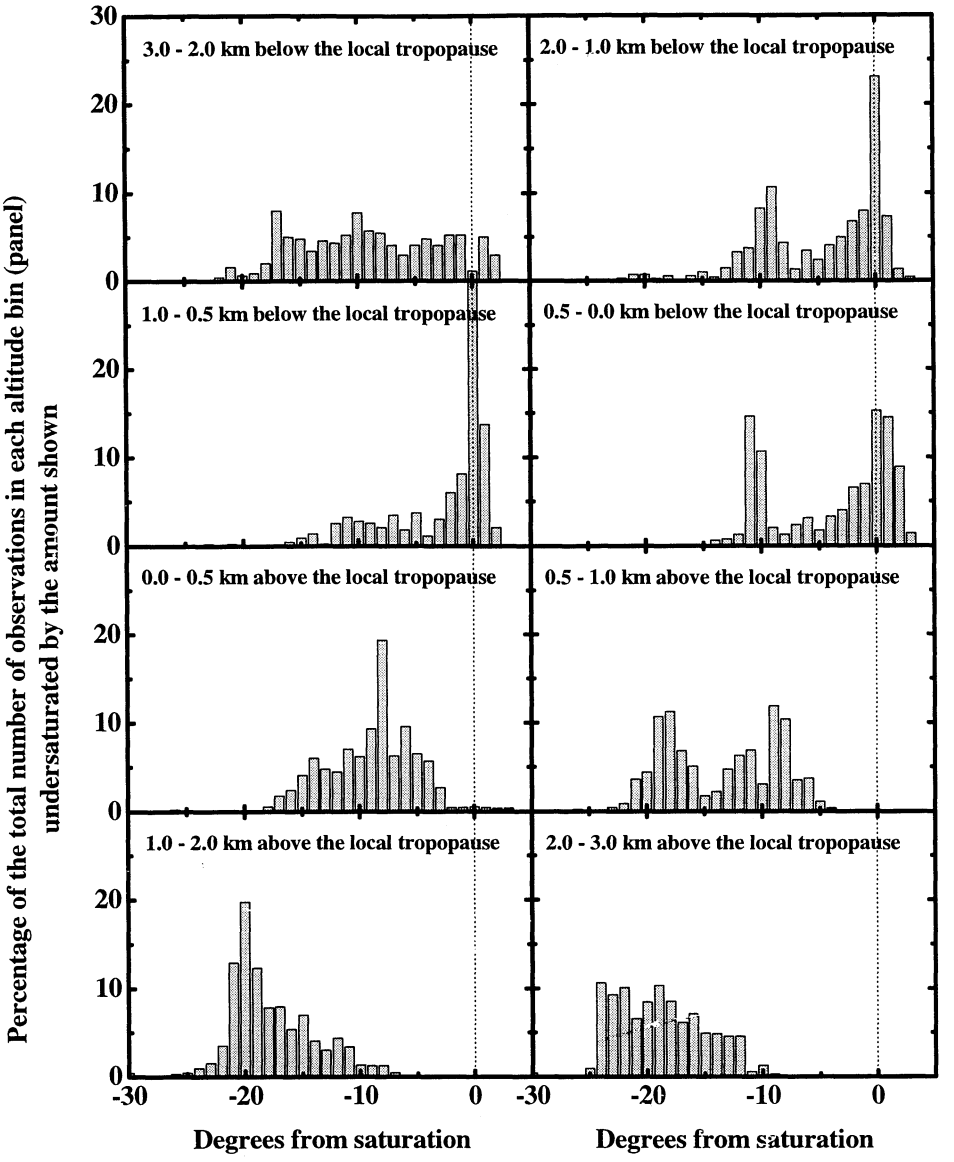

Figure 6. Histograms showing normalized distributions of measured degrees from saturation, $T_{saturation}$ - $T_{measured}$, for altitude bins ±3 km around the local tropopause. The resolution in the range ±1 km about the tropopause increases from 1 km altitude bins to 0.5 km bins.

occurrence frequency. In the transition region, ±1 km about the tropopause, we increase our altitude resolution by evaluating the histograms for 0.5 km bins instead of 1 km bins. The plot shows only midlatitude data. Below the tropopause the histograms peak at zero degrees separation; that is, the most probable temperature is the temperature of saturation. However, in the 0.5 km altitude bin just above the tropopause, the histogram peak shifts abruptly away from saturation, indicating the sharp onset of undersaturation in the lowermost stratosphere. The data show that the stratosphere is undersaturated by a minimum of 10 K only 2 km above the tropopause. Figure 7 shows the same trend. In this figure all the data in each altitude bin are plotted in a phase diagram, that is, measured water vapor partial pressure versus measured temperature. The water vapor/ice transition is the solid line in each plot. The majority of the data points lie along the saturation line just below the tropopause, but fall away from the line just above the tropopause. These plots, in combination with the backtrajectory calculations, underscore the fundamental observed characteristics of the thin layer immediately above the tropopause: (1) there is a sharp divergence between the observed temperature and the calculated temperature of saturation; and (2) air parcels within 10 K of saturation located in the first 3 km above the tropopause do not approach the saturation condition along backward (or forward) trajectories. The in situ observations reveal a sharply diminishing probability of ice saturation in the lower stratosphere, driven by a precipitous decrease in relative humidity.

The lowermost stratosphere, as defined in the introduction, is a region distinct from the rest of the stratosphere, or overworld [*Holton et al.*, 1995; *Dessler et al.*, 1995]. The water vapor mixing ratios observed in the lowermost stratosphere are notably higher than those of the overworld

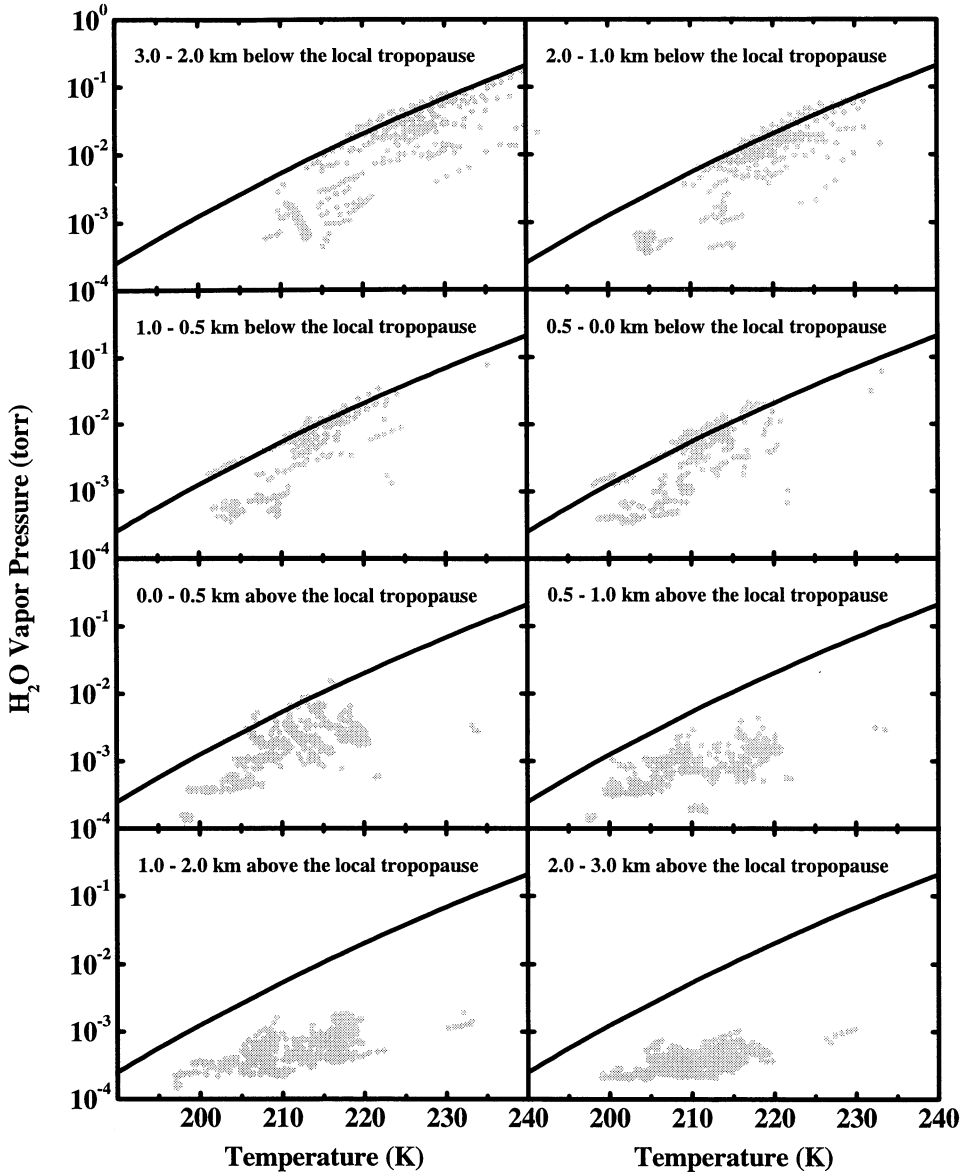

Figure 7. Phase diagram displaying the observed relationship between measurements of water vapor pressure and temperature referenced to the saturation line (solid line in plots) for altitude bins ranging ±3 km around the local tropopause. The resolution in the range ±1 km about the tropopause increases from 1 km altitude bins to 0.5 km bins.

[*Pan et al.*, 1997], but this analysis of in situ data shows they are not sufficient for ice saturation. Adiabatic transport along isentropic surfaces and/or vertical diabatic transport across isentropes to and from the troposphere influences the chemical properties of this region. In particular, water vapor concentrations in this region are consistent with a mixture of dry air from the overworld, determined primarily by the low temperatures encountered at the tropical tropopause, and moister air that has been transported isentropically with either tropical/subtropical or midlatitude origin [*Dessler et al.*, 1995, *Hintsa et al.*, 1998]. The mixing of dehydrated air from the overworld coupled with the temperature trend at the tropopause may explain the transition in relative humidity at the tropopause, and the observed scarcity of saturation events in the stratosphere. It has also been suggested that, regardless of their exact origin, air parcels with high water vapor mixing ratios have often reached saturation temperatures near the tropopause and have therefore undergone dehydration prior to their entry into the lowermost stratosphere and mixing there with drier air from the overworld [*Hintsa et al.*, 1998].

4.3. Comparison With the *Solomon et al.* [1997] Analysis on Cirrus

The success of the *Solomon et al.* [1997] model of heterogeneous chemistry on stratospheric cirrus is contingent upon an accurate representation of the frequency of cloud events. They used a seasonal climatology of cloud observations from SAGE II satellite data [*Wang et al.*, 1996] coupled with a climatological tropopause position to determine the frequency of cirrus cloud events in the midlatitude lowermost stratosphere. Their results yield summer cloud occurrence frequencies on the order of 1-10% at altitudes as high as 13-15 km, that is, above the average summer tropopause evaluated at 45°N [*Solomon et al.*, 1997].

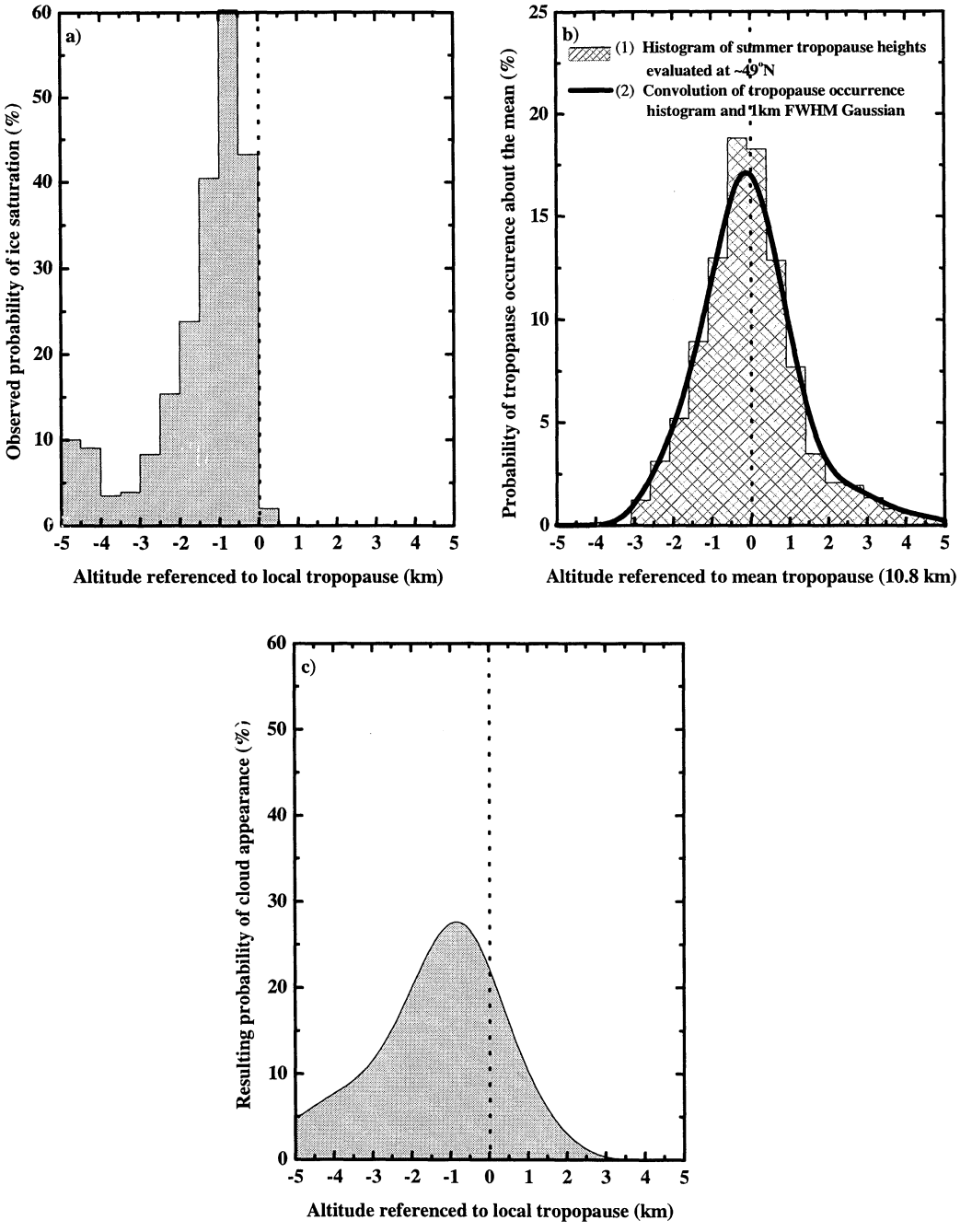

Figure 8. The convolution sequence showing (a) the high-resolution ER-2 observations of cloud occurrence frequency; (b) the spatial weighting function, evaluated at ~49°N, that results from the convolution of the "climatological smear," which is the result of assuming a climatological tropopause, and a Gaussian representing the intrinsic vertical resolution of the SAGE II satellite; and (c) the resulting distribution of cloud occurrence frequency in the lower stratosphere, obtained by the convolution of Figures 8a and 8b.

The effect of these clouds on modeled ClO was summarized in Figures 2 and 3. The high-resolution ER-2 observations suggest a very different picture. First, when keyed to simultaneous observations of tropopause position, the probability for cirrus cloud occurrence in the midlatitude stratosphere drops to a few percent in the first 0.5 km above the tropopause, and to immeasurably low levels above that. Second, the altitude of the tropopause varies markedly on short timescales, with the tropopause altitude shifting by 2-3 km about its mean.

Thus we consider the following issue: Suppose the observed high-resolution distribution of cirrus cloud frequency is convolved with a function which represents both the intrinsic vertical resolution of the SAGE II instrument (~1 km full width at half its maximum observational sensitivity) and the "climatological smear" resulting from the observed short-term vertical translation of the actual tropopause height about its climatological mean. What then is the inferred cloud occurrence frequency? To test this, we derived a spatial weighting function comprised of a Gaussian

function, measuring 1 km full width at half maximum, convolved with a normalized histogram of the frequency of tropopause occurrence above and below its average value. The histogram was evaluated using temperature and pressure altitude measurements from a compilation of radiosonde data from the summer season, and the WMO tropopause definition (P. Newman, private communication, 1999). The data were selected to be coincident with the ER-2 missions, that is, from 1995 to 1997, and were chosen from a narrow band centered at ~49°±1°N at all longitudes to best compare with the cloud occurrence frequencies inferred by *Solomon et al.* [1997]. Compare their Figures 3 and 7. The subsequent convolution of the spatial weighting function with the observed high-resolution cloud occurrence data from the ER-2 yields an enhanced distribution of cloud frequency in the lower stratosphere. This sequence is shown explicitly in Figure 8. The convolution processes conserve the area under the original curve; that is, the integrated cloud occurrence frequency is a constant. The largest effect results, of course, from the "climatological smear," since that assumption dominates the spatial weighting function. The combined result yields inferred occurrence frequencies above the tropopause markedly greater that those actually observed in the high-resolution data. The low resolution resulting from the combination of the vertical resolution of the remote sensing technique, in combination with a tropopause height locked to the climatological mean, operates to "create" reactive surface area in the lower stratosphere.

Midlatitude tropopause data from the ER-2 reveal a strong bimodal distribution. This is a result of the fact that nearly all the tropopause data are centered at 38°N (above NASA Ames), a latitude range where the tropopause altitude has a strong seasonal dependence, that is, a higher "summer" (subtropical) tropopause, from northward excursions of the subtropical jet, and a lower "winter" (midlatitude) tropopause. The highest tropopause values are found in summer, with some observations showing a tropopause nearly as high as in the tropics/subtropics (360-380 K potential temperature, ~16 km). The bimodal character is reproduced in histograms of NCEP radiosonde data from sites selected for their proximity to NASA Ames. Use of summer ER-2, or radiosonde data centered at 38°N in a calculation similar to that shown in Figure 8, further increases the relative cloud occurrence above the tropopause due to the broader distribution of tropopause heights at this latitude.

The seasonal variation of cirrus cloud frequency reported by *Solomon et al.* [1997], in particular the increased frequency of cloud observations in summer, is most likely another artifact of using a climatological tropopause. As mentioned above, data from the midlatitude ER-2 flights show that the position of the summer tropopause has a wide dynamic range. Using a fixed climatological tropopause will not reflect the frequently lifted local tropopause values in summer and will overestimate stratospheric cloud events in that season. Analysis of the midlatitude ER-2 data showed that all 26 data points that showed evidence of saturation in the first 0.5 km bin above the tropopause, of a total 1268 observations in that bin, occurred between December and mid-May, and 21 of the 26 occurred between December and the beginning of February. Furthermore, observation of saturation events in the winter season is consistent with the results of *Murphy et al.* [1990]. Their analysis of ER-2 data taken over Moffett Field, California (37°N) and Wallops Island, Virginia (31°N) yields evidence of saturation just above the tropopause in the winter season, but none in summer.

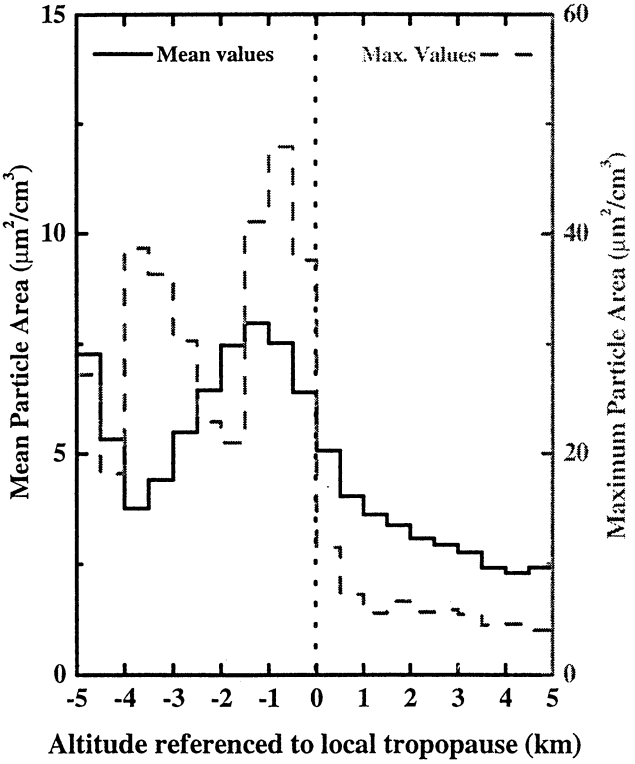

Figure 9. Observed particle surface area as a function of altitude referenced to the local tropopause. The mean values for each bin are represented by the solid curve, and the dashed curve is a plot of the maximum observed value in each bin. Note the mean and maximum plots use the left and right y axes, respectively; also, mean values in this figure and all subsequent figures are the bin-wise averages of individually calculated values.

4.4. Particle Reactive Surface Area

Particle reactive surface area is critical because the rate constant defining the heterogeneous conversion of inorganic chlorine to free radical form is given by $k_{het} = (v/4)\gamma S_a$, where v is the average molecular speed, γ is the reaction probability per collision, and S_a is the available aerosol/cirrus cloud reactive surface area. Particle surface area was measured aboard the ER-2 by an array of instruments [*Jonsson et al.*, 1995]. The data were again dissected by latitude and altitude in 0.5 km bins keyed to the local tropopause. We averaged all the data bin-wise and recorded the highest observed value of S_a in each altitude bin. These results are displayed in Figure 9. The mean measured particle surface area peaks just below the tropopause, and decreases steadily above it. The maximum observed surface area drops dramatically, and the distribution of particle areas narrows sharply at the tropopause. Reaction probabilities on these aerosol surfaces and their impact on halogen partitioning are discussed below.

4.5. Reaction Probability on Cold Aerosols

The possibility that heterogeneous reactions occur on aerosol particles, not strictly cirrus clouds, in the lowermost stratosphere is suggested as an alternative mechanism for the

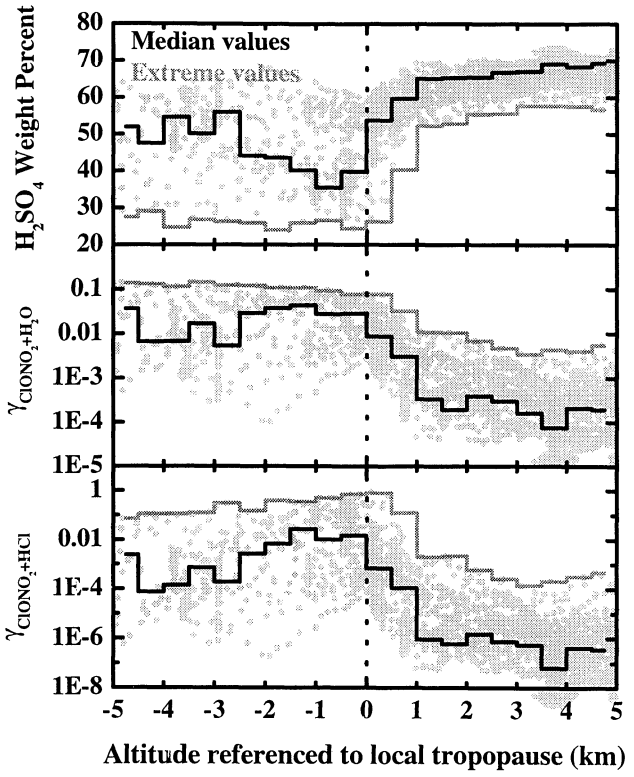

Figure 10. Calculated H_2SO_4 weight percents, and reaction probabilities, γ, for the heterogeneous activation of chlorine by reaction of $ClONO_2$ with H_2O and with HCl as a function of height about the tropopause, determined using simultaneous observations of temperature, pressure, H_2O, HCl, and calculated H_2SO_4 weight percent. Where measured HCl was not available below and just above the tropopause we used a constant value of 100 pptv. The bin-wise median and extreme values are the solid curves.

ozone loss observed at midlatitudes [*Solomon et al.*, 1996, 1998]. Aerosol surface area is a function of aerosol number density, temperature, pressure, and water vapor mixing ratio. Laboratory results defining the sharp increase of γ with decreasing temperature, in combination with model results, suggest that ice saturation is not required for heterogeneous chemistry to be significant [*Michelsen et al.*, 1999]. ER-2 in situ data allow for direct investigation of this question. We used measurements of temperature, pressure, and water vapor mixing ratio to calculate H_2SO_4 weight percents (adapted from *Carslaw et al.* [1995]). We used the H_2SO_4 weight percents along with simultaneous measurements of HCl [*Webster et al.*, 1994], water vapor mixing ratios, and particle surface area, and the parameterization of *Hanson* [1998], to calculate the corresponding reactive uptake coefficients for the heterogeneous reactions $H_2O + ClONO_2 \rightarrow HOCl + HNO_3$ and $HCl + ClONO_2 \rightarrow Cl_2 + HNO_3$ on sulfuric acid aerosols. We used measured HCl whenever it was reported. Where measurements were scant, at and below the tropopause, we used a default value of 100 pptv. The resulting data were then binned by latitude and altitude.

Figure 10 shows the results of our calculations for sulfuric acid weight percent and γ for midlatitudes. All the calculated values are plotted as a function of altitude about the local tropopause, with the median values for each bin and the relevant extreme values highlighted (minimum values for sulfuric acid weight percent, and maximum values for the γ values). The sulfuric acid weight percent decreases up to the tropopause and increases rapidly within the first kilometer above it. This is consistent with the increasing relative humidity and low temperatures just below the tropopause and the sudden transition to drier air above. The reaction probabilities γ, which are extremely sensitive to both temperature and water vapor mixing ratio, change dramatically as a function of distance above the tropopause. They are affected by sulfuric acid weight percent because the presence of sulfuric acid "poisons" the key heterogeneous reactions [e.g., *Kolb et al.*, 1996, and references therein; *Ravishankara et al.*, 1998]. Our results show that the chlorine activation potential on aerosols falls off by an order of magnitude or more just as the chlorine begins to emerge from the organic source molecules and where calculated ozone trends begin to be statistically significant, 1-2 km above the tropopause.

We calculated the time constants for both reactions using the reactive uptake coefficients γ, measured particle surface area S_a, and mean molecular speed calculated from the measured temperature. The first-order time constants for both reactions, shown in Figure 11, see a corresponding order of magnitude increase in the region just above the tropopause. The minimum calculated time constants for both reactions are significantly longer than the time constant for $ClONO_2$ photolysis >0.5 km above the tropopause. In sharp contrast,

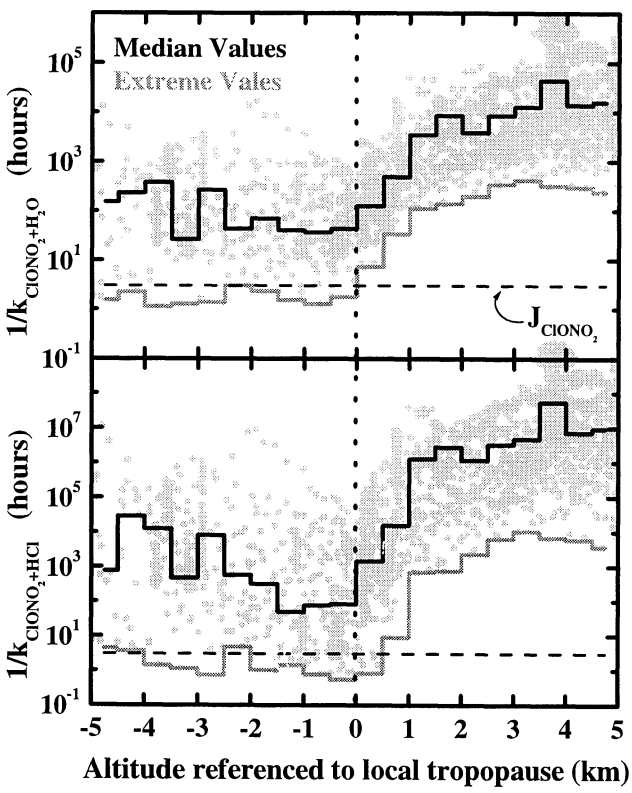

Figure 11. Calculated first-order time constants for the heterogeneous activation of chlorine by reaction of $ClONO_2$ with H_2O and HCl as a function of distance from the local tropopause, based on simultaneous observations of H_2O, HCl, and S_a and calculated γ values.

Solomon et al. [1997] estimate the time constants to be on the same order as photolysis, a few hours or less, for the lowermost stratosphere.

4.6. Observed Concentrations of ClO in the Vicinity of the Tropopause

A critical question remains: What evidence exists for the presence of enhanced concentrations of the rate limiting chlorine radical, ClO, in the lowermost stratosphere at midlatitudes? To this end, we analyzed ClO data from the most recent ER-2 aircraft missions that carried the Harvard ClO instrument, the Stratospheric Photochemistry, Aerosols and Dynamics Expedition (SPADE), the Airborne Southern Hemisphere Ozone Experiment/Measurements for Assessing the Effects of Stratospheric Aircraft (ASHOE/MAESA), and POLARIS. This instrument has a detection threshold of ~2 pptv in a 30-s sample at cruise altitude and a detection threshold of ~5 pptv in stair-step flights or ascent/descent flights in the vicinity of the tropopause. In most cases, longer integration times are available, improving the detection limit. We examined all midlatitude (30°-50°N and S) ClO data that were within the first 4 km above the measured tropopause, only excluding volume elements that showed the distinct signature of vortex processing, that is, where the simultaneously measured N_2O was less than 250 ppbv. In all there are 1210 midlatitude data points from 56 flights.

Plate 2 shows the results of our analysis. Plate 2a shows all the midlatitude data in black, except that of the April 30, 1993, SPADE flight which is discussed below. The data for all latitudes, in total 2661 data points, are shown in the background for comparison. The mean for each 0.5 km bin is plotted in green; the standard error associated with each mean is covered by the size of the dot. The first result that emerges from the data set is that the ClO mole fraction in the vicinity of the tropopause appears evenly distributed about zero. We are unable to distinguish between 0.1 and 1 or 2 pptv because of the detection threshold of the measurement, and the possibility remains that ClO levels are slightly elevated above zero in the lowermost stratosphere. However, we can distinguish between a few pptv and the levels of ClO required to substantially increase the photochemical loss rate of ozone in the critical region from the tropopause to >3 km above it. In comparison with *Solomon et al.* [1997, Figure 14], where the model with cirrus clouds shows a diurnal average of 10 pptv ClO at 12 km, this data set does not show evidence for ClO enhancements of this order.

The ClO data from the SPADE flights of 1993, during which there was a large enhancement in background aerosol loading from the eruption of Mount Pinatubo, show one outstanding example of an enhanced ClO layer above the tropopause. *Keim et al.* [1996] reported ClO mixing ratios of 90 pptv ~0.5 km above the midlatitude tropopause, and attributed them to reactions on cold aerosols, in conjunction with moderate levels of observed water vapor. Plate 2b highlights the data from this flight in red. The plate demonstrates that the ClO instrument will detect significant enhancements of ClO near the tropopause. This phenomenon was not observed again in any of the other SPADE flights, or in >40 midlatitude flights following the decay of the Pinatubo aerosol. Furthermore, D.W. Toohey (personal communication, 1999) analyzed data from 1991-1992 and found no evidence of enhanced ClO near the midlatitude tropopause. If judged by the frequency of such observations, the event highlighted in Plate 2b must be considered exceedingly rare.

Analysis of the limited degree of variability that [ClO] typically exhibits in the first few kilometers above the tropopause reveals a few factors which determine its concentration. First, the fraction of organic chlorine released into inorganic form is both small and tightly coupled to the long-lived tracer field [see *Woodbridge et al.*, 1995; *Bonne et al.*, 2000] in the midlatitude tropopause region. Second, the product of the gradient in maximum reactive surface area, S_a, above the tropopause (Figure 9) and the "poisoning" of the key heterogeneous reactions that results from the increase in H_2SO_4 weight percent in the cold aerosols, strongly constrains the release of ClO from total available chlorine.

5. Summary and Conclusions

ER-2 flights extending over a period of 4 years provide simultaneous, high-resolution observations of (1) tropopause height; (2) ice saturation (a proxy for cloud occurrence) frequency in 0.5 km bins from 5 km below the tropopause to 5 km above the tropopause; (3) the degree of undersaturation in the same array of altitude bins; (4) particle reactive surface area S_a in the bins; (5) reaction probability on cold aerosols, γ; and finally (6) ClO concentrations. The observations reveal a sharply diminishing probability of observed ice saturation in the lower stratosphere, as well as a rapid decrease in γ for two representative chlorine activation reactions, driven by the sharp decrease in relative humidity and the resulting poisoning of the heterogeneous reactions by sulfuric acid. In summary, the atmospheric conditions that would enable these reactions exist with negligible frequency in the lowermost stratosphere. Finally, high-resolution observations of ClO show the absence of substantially enhanced chlorine radical concentrations in the first few kilometers above the local tropopause. These observations, obtained in situ by the ER-2, lead us to conclude that the observed losses of ozone at midlatitudes do not occur locally in the stratosphere via the heterogeneous partitioning of inorganic chlorine into free radical form as a result of cirrus or cold aerosols.

Acknowledgments. We thank Paul Wennberg for his gifted ideas and useful discussions, Bruce Gary for the tropopause data and many helpful comments, Paul Newman and Andy Dessler for assistance with radiosonde data, Ross Salawitch for his aid with rate calculations, and the pilots and crew of the ER-2 aircraft. This work was supported in part by the NASA Upper Atmospheric Research Program grant NAG-1-2007.

References

Anderson, J. G., W. H. Brune, and D. W. Toohey, Free radicals within the Antarctic vortex: The role of CFCs in Antarctic ozone loss, *Science*, *251*, 39-46, 1991.

Beyerle, G., H. J. Schafer, R. Neuber, O. Schrems, and I. S. McDermid, Dual wavelength lidar observation of tropical high-altitude cirrus clouds during the ALBATROSS 1996 campaign, *Geophys. Res. Lett.*, *25*, 919-922, 1998.

Bojkov, R. D., and V. E. Fioletov, Changes of the lower stratospheric ozone over Europe and Canada, *J. Geophys. Res.*, *102*, 1337-1347, 1997.

Bonne, G. P., et al., An examination of the inorganic chlorine budget in the lower stratosphere, *J. Geophys. Res.*, *105*, 1957-1971, 2000.

Borrmann, S., S. Solomon, J. E. Dye, and B. P. Luo, The potential of cirrus clouds for heterogeneous chlorine activation, *Geophys. Res. Lett.*, *23*, 2133-2136, 1996.

Borrmann, S., S. Solomon, L. Avallone, D. Toohey, and D. Baumgardner, On the occurrence of ClO in cirrus clouds and volcanic aerosol in the tropopause region, *Geophys. Res. Lett.*, *24*, 2011-2014, 1997.

Brune, W. H., J. G. Anderson, D. W. Toohey, D. W. Fahey, S. R. Kawa, R. L. Jones, D. S. McKenna, and L. R. Poole, The potential for ozone depletion in the Arctic polar stratosphere, *Science*, *252*, 1260-1266, 1991.

Carslaw, K. S., B. P. Luo, and T. Peter, An analytic expression for the composition of aqueous HNO_3-H_2SO_4 stratospheric aerosols including gas phase removal of HNO_3, *Geophys. Res. Lett.*, *22*, 1877-1880, 1995.

Del Negro, L. A., et al., Comparison of modeled and observed values of NO_2 and J_{NO2} during the Photochemistry of Ozone Loss in the Arctic Region in Summer (POLARIS) mission, *J. Geophys. Res.*, *104*, 26,687-26,703, 1999.

Denning, R. F., S. L. Guidero, G. S. Parks, and B. L. Gary, Instrument description of the airborne Microwave Temperature Profiler, *J. Geophys. Res.*, *94*, 757-765, 1989.

Dessler, A. E., E. J. Hintsa, E. M. Weinstock, J. G. Anderson, and K. R. Chan, Mechanisms controlling water vapor in the lower stratosphere: A tale of two stratospheres, *J. Geophys. Res.*, *100*, 23,167-23,172, 1995.

Fahey, D. W., et al., In situ measurements constraining the role of sulfate aerosols in midlatitude ozone depletion, *Nature*, *363*, 509-514, 1993.

Hanson, D. R., Reaction of $ClONO_2$ with H_2O and HCl in sulfuric acid and HNO_3/H_2SO_4/H_2O mixtures, *J. Phys. Chem. A*, *102*, 4794-4807, 1998.

Hintsa, E. J., et al., Troposphere-to-stratosphere transport in the lowermost stratosphere from measurements of H_2O, CO_2, N_2O and O_3, *Geophys. Res. Lett.*, *25*, 2655-2658, 1998.

Hintsa, E. J., E. M. Weinstock, J. G. Anderson, R. D. May, and D. F. Hurst, On the accuracy of in situ water vapor measurements in the troposphere and lower stratosphere with the Harvard Lyman-α hygrometer, *J. Geophys. Res.*, *104*, 8183-8189, 1999.

Holton, J. R., P. H. Haynes, M. E. McIntyre, A. R. Douglass, P. B. Rood, and L. Pfister, Stratosphere-troposphere exchange, *Rev. Geophys.*, *33*, 403-439, 1995.

Jensen, E. J., O. B. Toon, H. B. Selkirk, J. D. Spinhirne, and M. R. Schoeberl, On the formation and persistence of subvisible cirrus clouds near the tropical tropopause, *J. Geophys. Res.*, *101*, 21,361-21,375, 1996.

Jonsson, H. H., et al., Performance of a focused cavity aerosol spectrometer for measurements in the stratosphere of particle size in the 0.06-2.0 mm diameter range, *J. Atmos. Oceanic Technol.*, *12*, 115-129, 1995.

Keim, E. R., et al., Observations of large reductions in the NO/NO_y ratio near the midlatitude tropopause and the role of heterogeneous chemistry, *Geophys. Res. Lett.*, *23*, 3223-3226, 1996.

Kolb, C. E., D. R. Worsnop, M. S. Zahniser, and P. Davidovits, A spectroscopic tour through the liquid aerosol interface: Implications for atmospheric chemistry, *J. Geophys. Res.*, *101*, 23,039-23,043, 1996.

Logan, J. A., et al., Trends in the vertical distribution of ozone: A comparison of two analyses of ozonesonde data, *J. Geophys. Res.*, *104*, 26,373-26,399, 1999.

Michelsen, H. A., C. M. Spivakovsky, and S. C. Wofsy, Aerosol-mediated partitioning of stratospheric Cl_y and NO_y at temperatures above 200 K, *Geophys. Res. Lett.*, *26*, 299-302, 1999.

Murphy, D. M., K. K. Kelly, A. F. Tuck, M. H. Proffitt, and S. Kinne, Ice saturation at the tropopause observed from the ER-2 aircraft, *Geophys. Res. Lett.*, *17*, 353-356, 1990.

Pan, L. W., S. Solomon, W. J. Randel, J.-F. Lamarque, P. Hess, J. C. Gille, E.-W. Chiou, and M. P. McCormick, Hemispheric asymmetries and seasonal variations of the lowermost stratospheric water vapor and ozone derived from SAGE II data, *J. Geophys. Res.*, *102*, 28,177-28,184, 1997.

Pan, L. W., E. J. Hintsa, E. M. Stone, E. M. Weinstock, and W. J. Randel, The seasonal cycle of water vapor and saturation vapor mixing ratio in the extratropical lowermost stratosphere, *J. Geophys. Res.*, in press, 2000.

Poulida, O., R. R. Dickerson, and A. Heymsfield, Stratosphere-troposphere exchange in a midlatitude mesoscale convective complex, *J. Geophys. Res.*, *101*, 6823-6836, 1996.

Ravishankara, A. R., G. Hancock, M. Kawasaki, and Y. Matsumi, Photochemistry of ozone: Surprises and recent lessons, *Science*, *280*, 60-61, 1998.

Rinsland, C. P., et al., ATMOS/ATLAS 3 infrared profile measurements of clouds in the tropical and subtropical upper troposphere, *J. Quant. Spectrosc. Radiat. Transfer*, *60*, 903-919, 1998.

Rosenlof, K. H., and J. R. Holton, Estimates of the stratospheric residual circulation using the downward control principle, *J. Geophys. Res.*, *98*, 10,465-10,479, 1993.

Scott, S. G., T. P. Bui, K. R. Chan, and S. W. Bowen, The Meteorological Measurement System on the NASA ER-2 aircraft, *J. Atmos. Oceanic Technol.*, *7*, 525-540, 1990.

Solomon, S., R. W. Portmann, R. R. Garcia, L. W. Thomason, L. R. Poole, and M. P. McCormick, The role of aerosol variations in anthropogenic ozone depletion at northern midlatitudes, *J. Geophys. Res.*, *101*, 6713-6727, 1996.

Solomon, S., S. Borrmann, R. R. Garcia, R. Portmann, L. W. Thomason, L. R. Poole, D. Winker, and M. P. McCormick, Heterogeneous chlorine chemistry in the tropopause region, *J. Geophys. Res.*, *102*, 21,411-21,429, 1997.

Solomon, S., R. W. Portmann, R. R. Garcia, W. Randel, F. Wu, R. Nagatani, J. Gleason, L. W. Thomason, L. R. Poole, and M. P. McCormick, Ozone depletion at midlatitudes: Coupling of volcanic aerosols and temperature variability to anthropogenic chlorine, *Geophys. Res. Lett.*, *25*, 1871-1874, 1998.

Stimpfle, R. M., et al., The coupling of $ClONO_2$, ClO, and NO_2 in the lower stratosphere from in situ observations using the NASA ER-2 aircraft, *J. Geophys. Res.*, *104*, 26,705-26,714, 1999.

Toohey, D. W., L. M. Avallone, L. R. Lait, P. A. Newman, M. R. Schoeberl, D. W. Fahey, E. L. Woodbridge, and J. G. Anderson, The seasonal evolution of reactive chlorine in the northern hemisphere stratosphere, *Science*, *261*, 1134–1136, 1993.

Wang, P. H., P. Minnis, M. P. McCormick, G. S. Kent, and K. M. Skeens, A 6-year climatology of cloud occurrence frequency from Stratospheric Aerosol and Gas Experiment II observations (1985-1990), *J. Geophys. Res.*, *101*, 29,407-29,429, 1996.

Weast, R. C. (Ed.), *CRC Handbook of Chemistry and Physics*, 54th ed., CRC Press, Boca Raton, Fla., 1973.

Webster, C. R., R. D. May, C. A. Trimble, R. G. Chave, and J. Kendall, Aircraft (ER-2) Laser Infrared Absorption Spectrometer (ALIAS) for in situ stratospheric measurements of HCl, N_2O, CH_4, NO_2, and HNO_3, *Appl. Opt.*, *33*, 454-472, 1994.

Wennberg, P. O., R. C. Cohen, R. M. Stimpfle, D. W. Fahey, C. R. Webster, R. J. Salawitch, M. H. Proffitt, K. R. Chan, J. G. Anderson, and S. C. Wofsy, The removal of lower stratospheric ozone by free radical catalysis: In situ measurements of OH, HO_2, NO, NO_2, ClO, and BrO, *Science*, *266*, 398-404, 1994.

Winker, D. M., and C. R. Trepte, Laminar cirrus observed near the tropical tropopause by LITE, *Geophys. Res. Lett.*, *25*, 3351-3354, 1998.

Woodbridge, E. L., et al., Estimates of total organic and inorganic chlorine in the lower stratosphere from in situ and flask measurements during AASE-II, *J. Geophys. Res.*, *100*, 3057-3064, 1995.

N. T. Allen, J. G. Anderson, J. B. Smith, and R. M. Stimpfle, Department of Chemistry and Chemical Biology, Harvard University, 12 Oxford St., Cambridge, MA 02138. (jsmith@huarp.harvard.edu)

E. J. Hintsa, Department of Marine Chemistry and Geochemistry, Woods Hole Oceanographic Institution, Woods Hole, MA 02543.

(Received August 13, 1999; revised July 31, 2000;
accepted August 2, 2000.)